Appl. Phys. B 77, 125–128 (2003)
DOI: 10.1007/s00340-003-1254-z

Applied Physics B
Lasers and Optics

T. FUJI[1,✉]
A. UNTERHUBER[2]
V.S. YAKOVLEV[1]
G. TEMPEA[1]
A. STINGL[3]
F. KRAUSZ[1]
W. DREXLER[1,2]

Generation of smooth, ultra-broadband spectra directly from a prism-less Ti:sapphire laser

[1] Photonics Institute, Christian Doppler Laboratory, Vienna University of Technology, Gusshausstrasse 27/387, 1040 Vienna, Austria
[2] Department of Medical Physics, Christian Doppler Laboratory, University of Vienna, Währingerstrasse 13, 1090 Vienna, Austria
[3] FEMTOLASERS Produktions GmbH, Fernkorngasse 10, 1100 Vienna Austria

Received: 25 April 2003/Revised version: 10 June 2003
Published online: 25 July 2003 •

ABSTRACT Ultra-broad and smooth spectra are generated directly from a mirror-dispersion-controlled Kerr-lens mode-locked Ti:sapphire oscillator. The full width at half maximum of the spectrum is 277 nm. The pulse width is evaluated as 6.5 fs by using both interferometric autocorrelation and spectral phase interferometry for electric-field reconstruction. This compact, user-friendly source opens the door to routine implementation of ultra-high-resolution as well as spectroscopic optical coherence tomography in a clinical environment.

PACS 42.60.By; 42.65.Re

1 Introduction

The range of applications of femtosecond Ti:sapphire lasers is constantly broadening and penetrates increasingly into industrial technologies and medical techniques. The production of ultra-short laser pulses continues to be a very active field of research. This technology has found applications in the areas of biological imaging, micromachining, high-speed communications, and the investigation of ultrafast carrier dynamics in semiconductor devices. For many applications, not only shortness of the pulses but also a Gaussian spectral distribution with minimal ripple and modulation are important. Optical coherence tomography (OCT) is one of the most promising real-world applications of ultra-broadband Ti:sapphire oscillators. The instrumental function of OCT is defined by the inverse Fourier transform of the spectrum of the light source; therefore the OCT resolution is determined by the spectral width of the light source. A strongly structured spectrum will produce side lobes in the OCT interferogram that will result in poor image quality due to artifacts.

The broadest spectra from a mode-locked Ti:sapphire laser have so far been obtained by combined use of prisms, chirped mirrors, and a glass plate for enhanced self-phase modulation [1]. Recently, broad spectra due to self-phase modulation in a Ti:sapphire crystal have also been demonstrated from a prism-less oscillator [2, 3]. However, in both cases the laser spectrum is strongly modulated, severely compromising applications where a clean temporal structure of the generated pulses or the first-order autocorrelation of the laser output is essential. The latter requirement applies to ultra-high-resolution and spectroscopic OCT [4, 5].

In this Letter, we report the generation of ultra-broadband and smooth spectra from a prism-less Ti:sapphire laser for the first time. The laser is formed by a standard x-folded resonator [6] composed of chirped mirrors, a broadband output coupler, and a pair of wedges for fine tuning the dispersion in the cavity. A major advantage of the prism-less laser is the compactness and stability of the cavity, which are essential for biomedical OCT application in clinical studies and for carrier-envelope phase stabilization [7]. The generated spectrum has a 277 nm bandwidth at full width at half maximum (FWHM) and with only 2 dB spectral modulation. In addition, the spectral bandwidth is ~ 380 nm at -10 dB below its maximum, which is suitable for phase stabilization and frequency metrology based on interference of second- and third-harmonic light [8, 9].

The schematic of the laser cavity is shown in Fig. 1. The laser is pumped by a diode-pumped, frequency-doubled

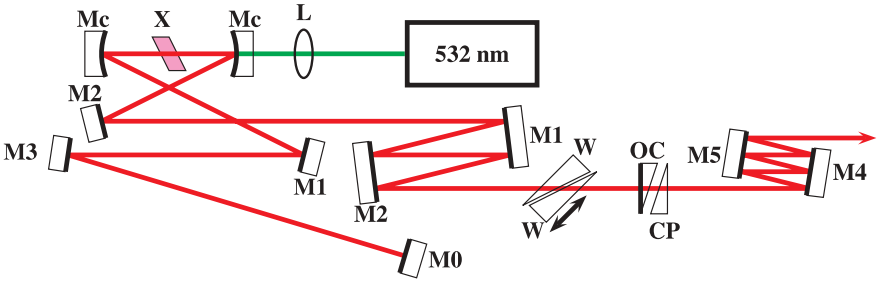

FIGURE 1 The schematic of the prism-less Ti:sapphire laser and extracavity dispersion-compensation setup. CP: compensating plate; L: incoupling lens; M0–5: chirped mirrors; Mc: 50 mm folding mirror; OC: output coupler; X: Ti:sapphire crystal; W: wedged plate

✉ Fax: +43-1/58801-38799, E-mail: fuji@tuwien.ac.at

Nd:YVO_4 laser (Verdi, Coherent). The thickness and the absorption coefficient of the Ti:sapphire crystal are 2.5 mm and 5.0 cm^{-1}, respectively. The radius of curvature of the concave mirrors is $r = -50$ mm. All chirped mirrors in the cavity were designed by our group and manufactured by Layertec GmbH. The transmission of the output coupler is 10%. A pair of thin fused-silica wedges is inserted at the Brewster angle for intracavity dispersion control. The prismless laser generates an average output power of 250 mW for 3.65 W pump power and 64 MHz repetition rate.

The group-delay dispersion (GDD) of each mirror, the net GDD in the cavity, and the resultant reflectivity of all high reflectors and the output coupler are shown in Fig. 2a, b, and c, respectively. We use four types of chirped mirrors. One (Mc and M0) is specifically designed for the input coupler for a 532 nm pump beam. To compensate the fluctuation of GDD of the input coupler, we use other two types of mirrors (M1 and M2). Additionally, we have inserted one chirped mirror (M3) in the cavity to introduce a negative third-order dispersion (TOD, $\sim 130\,fs^2$ per bound) in addition to negative GDD to compensate for the positive TOD contributions from other intracavity components (Ti:sapphire crystal and wedges). In the absence of this TOD control, a sharp spectral feature appears at short wavelength (near 700 nm). Our tests show that controlling the TOD is more critical for the generation of smooth output spectra with minimal spectral fluctuations than a full suppression of GDD fluctuations.

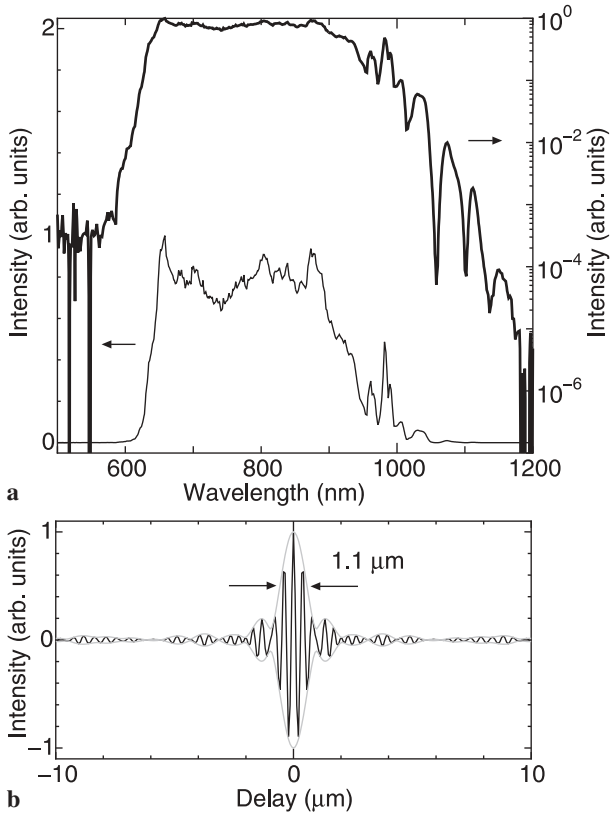

FIGURE 3 **a** The spectrum generated from the mirror-dispersion-controlled oscillator depicted on a logarithmic and a linear scale. **b** Linear autocorrelation trace obtained by inverse Fourier transform of the spectrum

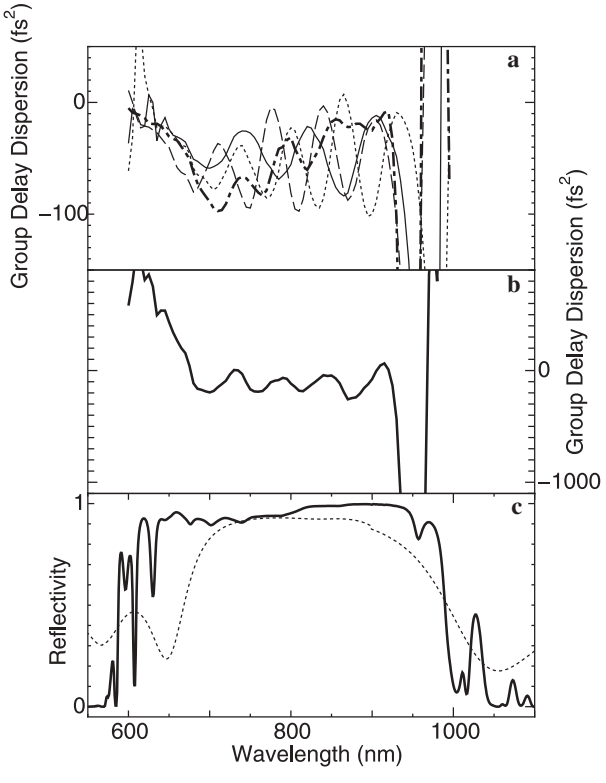

FIGURE 2 **a** Group-delay dispersion (GDD) per bounce of the mirrors M0 and Mc (*solid line*), M1 (*dotted line*), M2 (*dashed line*), and M3 (*dot-dashed line*) in the cavity. The position of each mirror is shown in Fig. 1. **b** Net intracavity GDD. **c** The resultant reflectivity of high-reflecting mirrors upon one round trip in the cavity (*full line*) and that of the 10% output coupler (*dotted line*)

The spectrum generated from the oscillator and measured with an optical spectrum analyzer (AQ-6315A, Andor Technology) with single monochromator mode is shown in Fig. 3a in linear as well as logarithmic representations. The bandwidth of the spectrum is 277 nm (141 THz) FWHM. The fine spectral modulations at long wavelengths are caused by vapor absorption and/or the structure of the reflectivity spectrum of the chirped mirrors in the cavity. On the logarithmic scale, spectral components can be observed at ~ 625 nm and 1005 nm at -10 dB below maximum. As a result the laser could be carrier-envelope-phase stabilized without any additional extracavity broadening system with the $2f$–$3f$ method [8, 9]. The linear autocorrelation trace obtained with the inverse Fourier transform of the spectrum is shown in Fig. 3b. Hence the laser would enable an OCT axial resolution of 1.1 μm in free space and 0.8 μm in biological tissue ($n = 1.4$).

Although the chirped mirrors and the output coupler only support a spectrum from 700 nm to 900 nm, the generated spectrum from the oscillator extends beyond this region. This means that most of the light at the wings of the spectrum is not generated through lasing but by self-phase modulation in the crystal, a phenomenon previously observed [2, 3, 10]. Further optimization of the bandwidth of the chirped mirrors and of the output coupler holds promise for generating even broader spectra in the future.

The output pulses are compressed by six reflections of the chirped mirrors, and the temporal characteristics of the pulses are measured using an interferometric autocorrelator designed for sub-10-fs pulse diagnostics (Femtometer, FemtoLasers). The frequency-doubling crystal is a 10-μm-thick β-BaB_2O_4 (BBO) crystal (Type I, $\theta = 29°$). The dots in Fig. 4 show the measured interferometric autocorrelation trace (IAC). The FWHM of the intensity envelope has been evaluated as 6.5 fs by using a phase-retrieval algorithm.

In order to characterize the spectral phase of the pulses more directly, spectral phase interferometry for electric-field reconstruction (SPIDER) [11] was also used. It is necessary to characterize ultra-short pulses with both time-domain and frequency-domain methods [12]. The SPIDER spectrum has been measured by a spectrograph (model 77400, Oriel Instruments) employing a cooled CCD camera (DV420-OE, Andor Technology). The dispersive material used for stretching the pulses is a 5-cm thick SF57 glass slab. A 60-μm thick BBO crystal (Type II, $\theta = 42.7°$) is used for sum-frequency generation of the twin pulses and the stretched pulse. The measured SPIDER spectrum, the retrieved spectral phase, and the temporal profile are shown in Fig. 5a, b, and c, respectively. The oscillating structure of the GDD is clearly retrieved. The oscillation feature completely corresponds to the GDD oscillation of the compressor shown as a dotted line in Fig. 5b. The large slope in the short-wavelength region (∼ 670 nm) is due to higher-order dispersion of the output coupler. The reason for the accurate measurement is that the fringes can be easily resolved with such a smooth spectrum and the fine structure in the long-wavelength region is useful to calibrate the difference of the optical frequency in spectral sharing. The FWHM of the intensity envelope in the time domain is estimated as 6.5 fs, in accordance with the result of the IAC. The retrieved IAC from the SPIDER measurement is shown as a solid line in Fig. 4. The measured IAC trace and that retrieved from the SPIDER measurement are in good agreement.

The generated laser spectrum would allow 4.8-fs pulses if the chirp of the pulses could be fully eliminated. At present, the oscillating component of the GDD frustrates further pulse short-

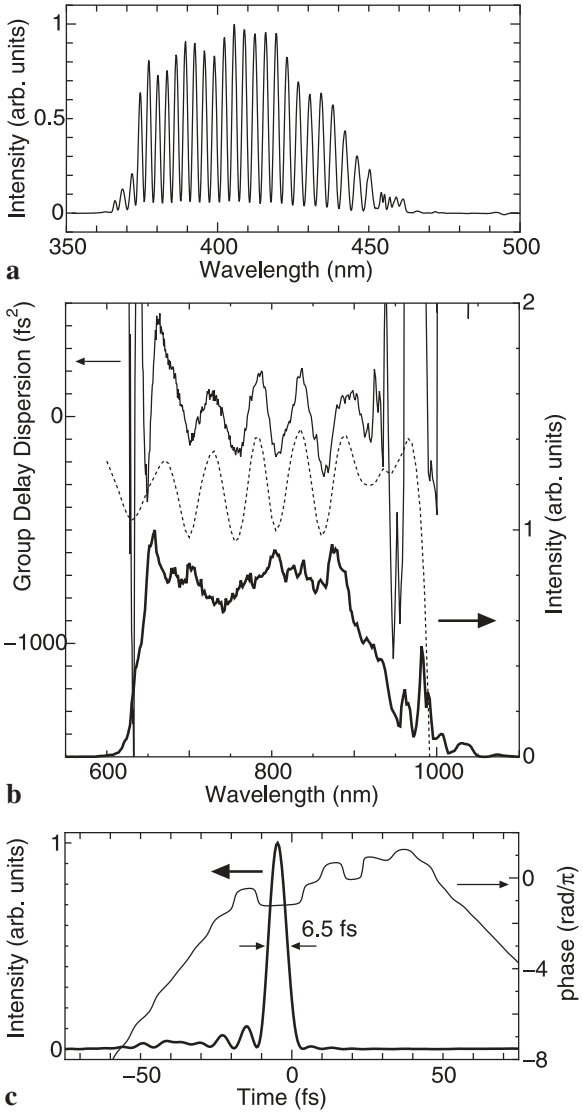

FIGURE 5 **a** The measured SPIDER spectrum. **b** Retrieved spectral phase and intensity spectrum of the pulses. *Dotted line* shows the group-delay dispersion of the compressor (M4 and M5 in Fig. 1) obtained with a white-light interferometer. **c** Intensity and phase of the pulses in the time domain

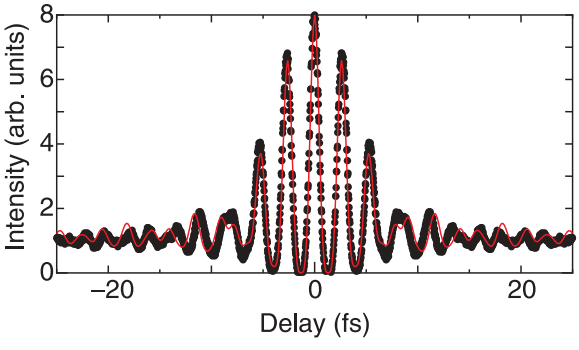

FIGURE 4 Measured and reconstructed interferometric autocorrelation traces of the pulse. A phase-retrieval algorithm reveals a pulse width of 6.5 fs. The *solid line* shows the retrieved IAC trace from a SPIDER measurement (Fig. 5)

ening. This way becomes feasible by the use of adaptive pulse compression [13].

In conclusion, we have demonstrated the generation of ultra-broad and smooth spectra from a compact mirror-dispersion-controlled Ti:sapphire oscillator. The FWHM of the spectrum is 277 nm. At −10 dB the spectrum extends from 625 nm to 1005 nm. The pulse duration is 6.5 fs. Owing to its compactness, reliability, and stability, the demonstrated source constitutes an ideal tool for ultra-high-resolution and spectroscopic optical coherence tomography.

ACKNOWLEDGEMENTS This work is supported by the Christian Doppler Society and FemtoLasers Produktions GmbH. T. Fuji also acknowledges support from JSPS Postdoctoral Fellowships for research abroad.

REFERENCES

1 R. Ell, U. Morgner, F.X. Kärtner, J.G. Fujimoto, E.P. Ippen, V. Scheuer, G. Angelow, T. Tschudi, M.J. Lederer, A. Boiko, B. Luther-Davies: Opt. Lett. **26**, 373 (2001)
2 A. Bartels, H. Kurz: Opt. Lett. **27**, 1839 (2002)
3 T.R. Schibli, L.M. Matos, F.J. Grawert, J.G. Fujimoto, F.X. Kärtner: 'Continuum generation in a prism-less Ti:sapphire laser'. In: R.D. Miller, M.M. Murnane, N.F. Scherer, A.M. Weiner (Eds.) *Ultrafast Phenomena XIII, Chemical Physics* (Springer, Berlin 2002) pp. 131–133
4 W. Drexler, U. Morgner, F.X. Kärtner, C. Pitris, S.A. Boppart, X.D. Li, E.P. Ippen, J.G. Fujimoto: Opt. Lett. **24**, 1221 (1999)
5 U. Morgner, W. Drexler, F.X. Kärtner, X.D. Li, C. Pitris, E.P. Ippen, J.G. Fujimoto: Opt. Lett. **25**, 111 (2000)
6 A. Stingl, M. Lenzner, Ch. Spielmann, F. Krausz: Opt. Lett. **20**, 602 (1995)
7 F.W. Helbing, G. Steinmeyer, J. Stenger, H.R. Telle, U. Keller: Appl. Phys. B **74**, S35 (2002)
8 U. Morgner, R. Ell, G. Metzler, T.R. Schibli, F.X. Kätner, J.G. Fujimoto, H.A. Haus, E.P. Ippen: Phys. Rev. Lett. **86**, 5462 (2001)
9 T.M. Ramond, S.A. Diddams, L. Hollberg, A. Bartels: Opt. Lett. **27**, 1842 (2002)
10 J.-P. Likforman, A. Alexandrou, M. Joffre: Appl. Phys. Lett. **73**, 2257 (1998)
11 C. Iaconis, I.A. Walmsley: IEEE J. Quantum Electron. **QE-35**, 501 (1999)
12 L. Gallmann, D.H. Sutter, N. Matuschek, G. Steinmeyer, U. Keller, C. Iaconis, I.A. Walmsley: Opt. Lett. **24**, 1314 (1999)
13 A. Baltuška, T. Fuji, T. Kobayashi: Opt. Lett. **27**, 306 (2002)